Role of Dihydrogen Bonds for the Stabilization of Self-Assembled Molecular Nanostructures

S. Blankenburg, E. Rauls,* and W. G. Schmidt

Lehrstuhl für Theoretische Physik, Universität Paderborn, 33095 Paderborn, Germany

Received: March 16, 2009; Revised Manuscript Received: May 4, 2009

We present first principles density functional theory calculations of three molecules, DEB and BuCYA, on a Au(111) surface. These molecules differ only in their side chains and have been observed to self-assemble in an ordered structure in the case of DEB but in a disordered structure in the case of BuCYA. Our calculations reveal the reason for this different behavior and explain recent STM-observations. The detailed analysis of the energetics underlines the importance of long-range dispersive interactions, which we find crucial to reproduce the experimental results.

Introduction

The autonomous ordering and assembly of atoms and molecules on atomically well-defined surfaces appears to be a very promising alternative route to even smaller functional systems with nanometer dimensions.[1,2] Covalent and noncovalent binding, hydrogen bonds, and the competing effects of intramolecular and molecule−surface interaction are the physical and chemical issues which open up a huge number of possibilities for structural design. However, the mechanisms controlling the self-ordering phenomena first need to be thoroughly understood in order to employ self-assembly and growth processes and to create taylor-made surface nanostructures. Thereby, the detailed analysis of prototypical, well-defined model systems from first-principles calculations is extremely helpful.[3−13]

In the particular context of noncovalent synthesis, the application of rosette molecules results in highly ordered and useful structures in 2D as well in 3D.[14−16] In this article, we present first principles density functional theory (DFT) calculations on the adsorption of cyanuric (CYA), diethylbarbituric (DEB), and butylcyanuric acid (BuCYA) on a Au(111) surface.

These three molecules are most suitable for a systematic investigation of the various interactions which drive self-organizing structure formation. They only differ by their side group and, thus, offer different hydrogen bond donor and hydrogen bond acceptor properties as well as steric hindrance properties related to longer or shorter side groups. Their flat geometry suggests only weak binding to the surface. As observed by scanning tunneling microscopy (STM),[17] the adsorption of the molecules on the Au(111) surface leads to rather different structures, the origin of which, however, is still unclear. While CYA and DEB form highly ordered hydrogen bonded surface networks, BuCYA shows only locally ordered structures. Deposition of CYA leads to a close-packed molecular network. DEB forms a chain-like overlayer, and BuCYA covers the surface with short segments of molecular chains and a few polygonal rings. Why does the variation of the functional group of the latter two molecules, the alkyl side chain, influence the adstructure formation decisively?

* To whom correspondence should be addressed. E-mail: rauls@phys.upb.de.

Theoretical Section

In order to answer this question and rationalize this fascinating example of molecular self-assembly, we performed DFT calculations with the Vienna ab initio simulation package (VASP).[18] The PW91 functional[19] was used to model the electron exchange and correlation interaction within the generalized gradient approximation (GGA). The electron-ion interaction was described by the projector-augmented wave (PAW) method,[20] which allows for an accurate treatment of the first-row elements as well as the Au 5d electrons with a relatively moderate energy cutoff of 340 eV. Due to the huge lateral extension of the supercells used for the modeling, the surface Brillouin zone sampling was restricted to the Γ point. The adsystem was modeled by periodically repeated slabs, containing two atomic Au layers, the adsorbed molecules and a vacuum region of 15 Å. In order to estimate the H-bond strength within Bader's topological paradigm,[21] we used a functional of the calculated charge density.[22] In the case of molecules weakly bonded to each other or to the surface, dispersion interaction, not accounted for in the GGA, may contribute a sizable percentage of the total interaction energy.[4] In order to account at least approximately for the influence of the van der Waals (vdW) interaction on the adsorption energetics, we extended our ab initio description by a semiempirical expression of the dispersion interaction[23] based on the London dispersion formula. This approach has proven to be successful in the description of similar systems.[24,25]

Results and Discussion

We start with the single molecule adsorption within a

$$\begin{pmatrix} 5 & 0 \\ -2 & 4 \end{pmatrix} \tag{1}$$

periodicity. Figure 2 shows the fully relaxed adsorption geometries for the three molecules. According to $E_{ad} = E_{tot} - E_{mol} - E_{substr}$, we have calculated the adsorption energies to be −0.49, −0.71, and −0.80 eV for CYA, DEB, and BuCYA, respectively. Here E_{tot}, E_{mol}, and E_{substr} refer to the energies of the total system, the molecule in the gas phase and the clean substrate, all fully relaxed. Here, we mention that the inclusion of four gold layers results in a constant increase of the adsorption energies of about 0.03 eV which gives an estimate of the error

10.1021/jp902337p CCC: $40.75
Published on Web 06/24/2009

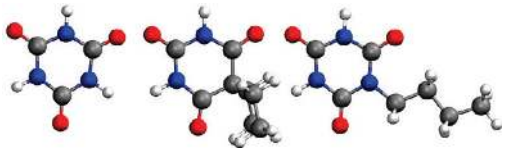

Figure 1. Ball and stick diagrams of CYA ($N_3C_3O_3H_3$), DEB ($N_2C_8O_3H_{12}$), and BuCYA ($N_3C_7O_3H_{11}$).

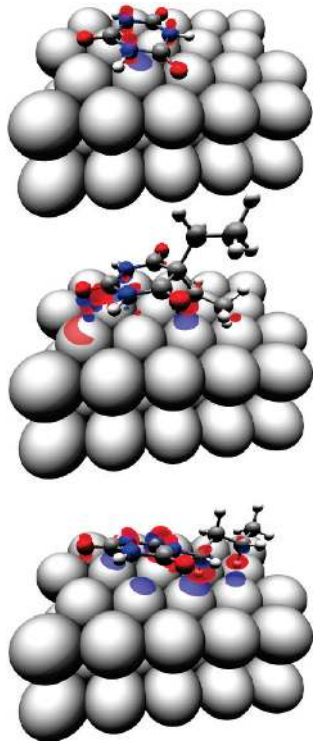

Figure 2. Adsorption geometries for CYA, DEB and BuCYA at Au(111). Charge accumulations are marked in blue, depletions in red (iso-surface value: 0.005 e/Å^3).

due to the use of just two layers. Excluding the van der Waals interaction leeds to a strong decrease in the adsorption strength with $E_{ad,CYA}^{DFT} = -0.06$ eV, $E_{ad,DEB}^{DFT} = -0.14$ eV, and $E_{ad,BuCYA}^{DFT} = -0.15$ eV, showing the importance of including dispersive interactions for this kind of systems. This is in accordance with Figure 2 that illustrates the charge density differences $\Delta\rho = \rho_{tot} - \rho_{mol} - \rho_{substr}$ representing the electronic redistribution upon adsorption. The small polarizations that can be seen support the proposition of vdW driven adsorption (cf. the small iso-surface value of 0.005 e/Å^3).

Turning now to more complex adsorption structures, we focus on DEB and BuCYA. CYA forms much simpler networks[17] that just serve as comparison for the more complex molecules in our investigations. The experimentally observed STM images[17] show highly ordered rows for DEB adsorption, while depositing BuCYA results in a local order, only. The BuCYA molecules assemble both to short segments of chains and to polygonal rings. In order to find out what causes this different behavior of the two molecules, we calculated chain-like molecular arrangements and six-membered ring structures for both molecules.

Starting from the experimental observations, our adsorption model for the DEB chains contains twelve molecules within a

$$\begin{pmatrix} 4 & 4 \\ 2 & 8 \end{pmatrix} \qquad (2)$$

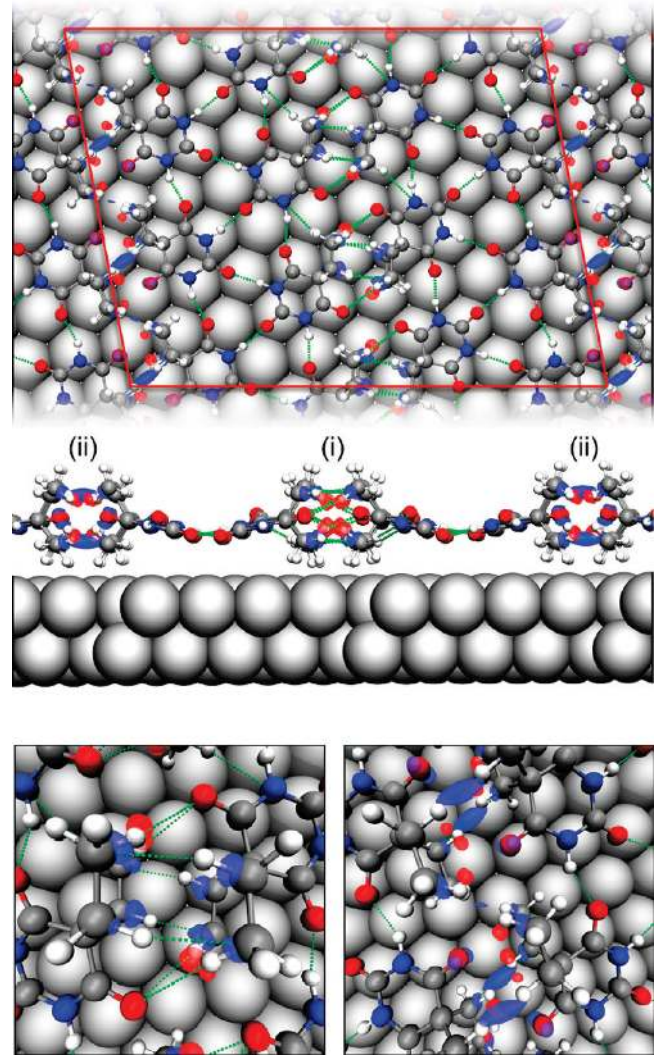

Figure 3. Chain structure of the DEB molecule with charge accumulation (blue) and depletion (red) due to the interaction between the chains (Iso-surface value: 0.008 e/Å^3). The surface periodicity is marked in red. Below, the dihydrogen bonding region of the above chain structure is shown in detail.

periodicity (72 Au atoms/layer). The structurally relaxed low-energy structure of the model together with the surface unit cell is shown in Figure 3 as top and side views.

Note that a complex network of hydrogen bonding evolves between the molecules (depicted with green dotted lines in Figure 3). In the following, we call two DEB molecules bonded with the CYA like rings together a chain. In neighboring chains, the molecular side chains face each other. As can be expected, the intrachain interactions are mediated by N−H···O H-bonds. But what accounts for the interchain interactions, which can be seen in Figure 3? The charge-density difference between the total system and the two separated chains reveals a complex interchain interaction. Two different borders exist between each chain and its neighbor chain: (i) the alkyl-side chains are nearly parallel and face each other, thus providing four C−H···C and two C−H···O H-bonds with a recognizable polarization, and (ii) the alkyl-side chains are also parallel but shifted along the chain direction, such that they do not face each other in neighboring chains. In the latter case, more C−H···H−C "bonds" can be observed with an electron accumulation between the protons. These nearly symmetric "dihydrogen bonds" are vastly dominated vdW-type interactions.[26,27] In order to assess

TABLE 1: Adsorption, Binding, Interaction and Deformation Energies per Molecule in eV for the Different Adsorption Models of DEB and BuCYA

mol.	struct.	E_{ad}	E_{bond}	$E_{WW,intra}$	$E_{WW,inter}$	E_{deform}
DEB	chain	−2.14	−0.64	−0.93	−0.66	0.10
BuCYA	chain	−1.54	−0.89	−0.87	−0.12	0.34
DEB	ring	−1.33	−0.62	−0.81		0.10
BuCYA	ring	−1.43	−0.93	−0.94		0.43

the strength of this interaction, we performed test calculations for a series of small alkanes. In the simple case of two C_2H_6 molecules, for example, the inclusion of vdW interactions results in an attractive force and an energy minimum with a similar electron accumulation between the protons as found above. The ab initio calculation without including vdW-terms yields $E_{WW}^{GGA} = 0.06$ eV, while the inclusion of vdW-interactions results in $E_{WW}^{GGA+vdW} = -0.22$ eV. This agrees well with the values obtained for similar systems in ref 27.

The calculated adsorption energy for the DEB chains amounts to −2.14 eV per molecule, thus being three times larger than for the single molecule adsorption. Resolving the adsorption energy into its components helps to understand the origin of this large increase: the binding energy that results from the pure chemical interaction with the surface, the inter- and the intrachain interaction energies and the deformation energy needed to distort the molecules from their gas phase geometry to their geometry in the adstructure. Table 1 shows these components. The binding energy accounts for 30%, the intrachain 44%, and the interchain interaction 30% of the total adsorption energy, thus indicating a stronger interaction between the molecules inside of the chains. Apparently, the binding energy to the surface decreases compared to the single molecule adsorption (0.71 eV) while the interaction energy reflects the largest contribution, and no strong deformation is needed to reach the favorable adsorption geometry.

According to the experiments,[9,17] the DEB molecule does not or only rarely form polygonal ring structures as observed for BuCYA. For our comparative calculations, we, thus, simply used a similar 6-membered polygonal ring structure as in the case of BuCYA. The left part of Figure 4 shows this structure within its

$$\begin{pmatrix} 9 & 0 \\ -5 & 10 \end{pmatrix} \quad (3)$$

surface periodicity (90 Au atoms/layer). Each molecule binds via two N−H···O H-bonds to each of its two neighbors. With −1.33 eV, the adsorption energy per molecule is by 0.81 eV smaller compared to that of the chain structure. At least for higher molecular densities in the adstructure, the ring structure

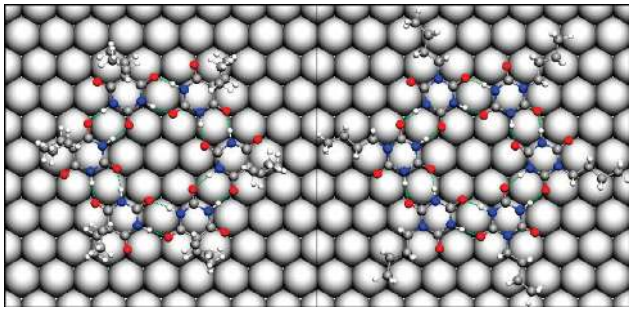

Figure 4. Six-membered ring structures for DEB and BuCYA. The size of each images is consitent with the cell periodicity.

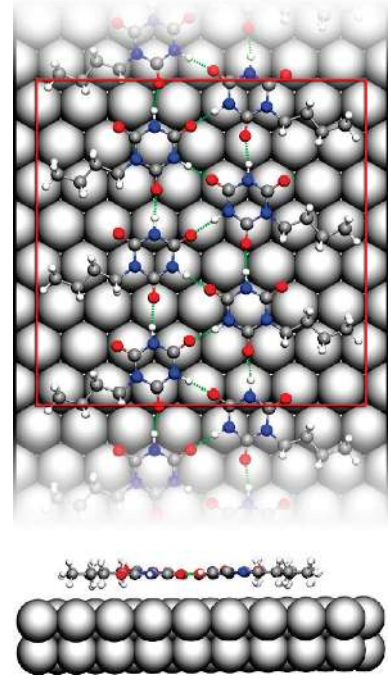

Figure 5. Chain structure of the BuCYA molecule with a top and side view. The surface periodicity ist marked in red.

represents, thus, an energetically rather unfavored overlayer. While the binding energy is −0.62 eV, i.e., comparable to that of the chain structure (−0.64 eV), the interaction energy shows a large decrease due to fewer interactions per molecule.

The BuCYA chain structure exhibits a

$$\begin{pmatrix} 7 & 0 \\ -4 & 8 \end{pmatrix} \quad (4)$$

periodicity (Figure 5, 56 Au atoms/layer). Like in the case of the DEB chains, the molecules form H-bonds inside and along the chains. In contrast to the DEB chains, however, only very weak interchain interactions via C−H···H−C "bonds" is observed. Inspite of a higher binding energy than in case of DEB, the overall adsorption energy is considerably lower. As could be expected, the intrachain interactions are comparable for both molecules, but the interchain interactions which to a large part stabilize the DEB chains are only about one-sixth. Additionally, the molecular strain involved in the adsorption of BuCYA is about three times larger than for DEB.

The 6-fold BuCYA ring structure is shown in the right part of Figure 4, again with a surface periodicity of

$$\begin{pmatrix} 9 & 0 \\ -5 & 10 \end{pmatrix} \quad (5)$$

The calculated adsorption energy is 0.1 eV lower than that of the BuCYA chains. For DEB, an energy difference of about 0.8 eV had been calculated for the two structures. That means that there is a clear preference for chain like structures in case of DEB, while we have to expect both adsorption structures in case of BuCYA. For higher molecular densities, i.e., a higher surface coverage, the chain structures will surely dominate and fill larger surface areas. The comparable adsorption energies of the ring structures, however, and the missing stabilization effects of the interchain hydrogen bonding in case of BuCYA prohibit a long-range order as observed for DEB.

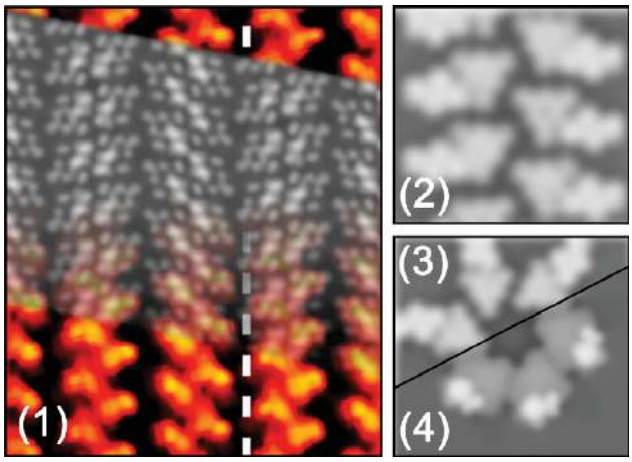

Figure 6. Calculated STM images for the chain structure of DEB (1), BuCYA (2), and the ring structures of BuCYA with a flat (3) and a folded side chain (4). The underlying experimental STM image in the case of DEB is taken from ref 17.

For a direct comparison to the experiment, we calculated constant current STM images (Figure 6) within the Tersoff-Hamann approximation.[28] As illustrated by the overlaid images in part (1) of Figure 6, the calculated and the experimental STM images agree very well for the DEB chain structure. Furthermore, this comparison shows that the characteristic bright spots are caused by the side chains of the DEB molecules. The brighter areas in the experimental image, thus, represent the interchain region (following our definition of a chain above), while there is a dark line in the experimental image along the center of the chains.

The calculated STM image for the BuCYA chain is shown in part (2) of Figure 6, the ring structure in part (3), respectively. An explanation for the bright spots in the experimental STM image to be more or less round and not as elongated as the BuCYA molecules suggest when adsorbed in the flat geometry might be that the flexible side chain is turned upward and across the CYA-like part of the molecule. The calculated STM image for a ring arrangement with molecules with an up-folded side chain agree quite well with the experimental STM image. In the gas phase, this molecular geometry is even preferred, and the energetical cost for folding the side chain into a flat configuration, amounts to 0.29 eV (cf. the deformation energy given in Tab. Table 1). The adsorption energy of −1.40 eV is comparable to that of the adsorption geometry discussed before.

Figure 7 shows superpositions of the calculated STM images for the two characteristic BuCYA aggregates on the experimental STM image, explaining both the chain-like and the ring-like patterns in the overall disordered arrangement.

Finally, we want to stress again the importance of including dispersive interactions. In Table 2, the respective values for the various components of the adsorption energies are given with and without dispersion interactions. In the latter case, binding and interaction energies decrease essentially for all structures, the molecule−surface interaction vanishes nearly completely. The main contribution to the adsorption energies stems from the H-bonds within the chains, while the interchain interaction turns to be a destabilizing factor, especially for the DEB chains. Here, we can also observe the strongest change in the results. While the energetical order of the BuCYA structures does not change when we neglect the vdW contributions, the DEB ring structure gets stabilized and the DEB chains become completely unstable. Apparently, the DEB chain structure, as observed experimentally, is only stabilized by the "dihydrogen bonds", which are of pure dispersive character and can, therefore, not be reproduced by ab initio calculations without consideration of dispersive interactions.

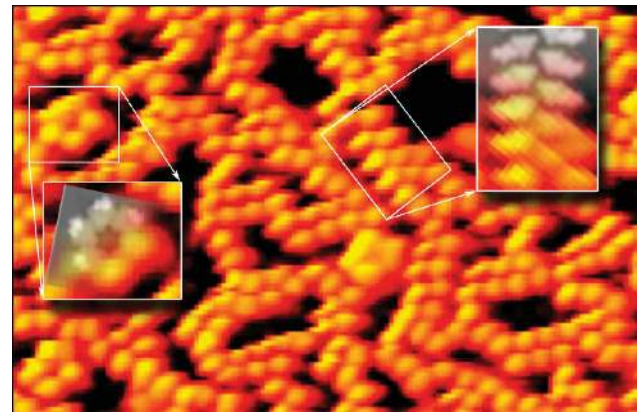

Figure 7. Calculated STM images for the chain and ring structure of BuCYA. The underlying experimental STM image is taken from ref 17.

TABLE 2: Adsorption, Binding, Interaction and Deformation Energies per Molecule in eV for the Different Adsorption Models of DEB and BuCYA Neglecting vdW Interactions

mol.	struct.	E_{ad}	E_{bond}	$E_{WW,intra}$	$E_{WW,inter}$	E_{deform}
DEB	chain	0.08	0.04	−0.36	0.25	0.15
BuCYA	chain	−0.41	−0.02	−0.61	−0.02	0.24
DEB	ring	−0.38	0.07	−0.63		0.18
BuCYA	ring	−0.36	−0.03	−0.67		0.35

Conclusion

In summary, we performed first principles density functional theory calculations in order to rationalize the influence of side-chains of two molecules, DEB and BuCYA, on their adsorption geometries on a Au(111) surface. Thereby, we could explain the different self-assembling behavior of DEB and BuCYA which had been observed in experimental STM investigations. The tendency of DEB to form perfectly ordered chainlike adstructures and, in contrast to this, the only local order of BuCYA with two competing adsorption geometries, could be explained by the different strengths of the various kinds of interactions which control the self-assembled structure formation. Detailed investigations of the charge transfer within the adstructure reveal that a special kind of H-bonds, i.e. "dihydrogen bonds", between the DEB side chains (C−H···H−C) play a major role in stabilizing the chain structure. This result could, though, only be obtained upon accounting for the long-range dispersive interactions, which commonly are neglected in DFT calculations.

Acknowledgment. The calculations were performed using grants of computer time from the Paderborn Center for Parallel Computing (PC^2) and the Höchstleistungs-Rechenzentrum Stuttgart. The Deutsche Forschungsgemeinschaft is acknowledged for financial support.

References and Notes

(1) Barth, J. V. *Annu. Rev. Phys. Chem.* **2007**, *58*, 375.
(2) Nilsson, A.; Pettersson, L. G. M. *Surf. Sci. Rep.* **2004**, *55*, 49.
(3) Hauschild, A.; Karki, K.; Cowie, B. C. C.; Rohlfing, M.; Tautz, F. S.; Sokolowski, M. *Phys. Rev. Lett.* **2005**, *94*, 036106.

(4) Ortmann, F.; Schmidt, W. G.; Bechstedt, F. *Phys. Rev. Lett.* **2005**, *95*, 186101.

(5) Langner, A.; Tait, S. L.; Lin, N.; Chandrasekar, R.; Ruben, M.; Kern, K. *Angew. Chem. -Int. Ed.* **2008**, *47*, 8835.

(6) Pennec, Y.; Schiffrin, W. A. A.; Weber-Bargion, A.; Rieman, A.; Barth, J. V. *Nat. Nanotechnol.* **2007**, *212*, 99.

(7) Ferretti, A.; Baldacchini, C.; Calzolari, A.; Felice, R. D.; Ruini, A.; Molinari, E.; Betti, M. G. *Phys. Rev. Lett.* **2007**, *99*, 046802.

(8) Mamdouh, W.; Dong, M.; Xu, S.; Rauls, E.; Besenbacher, F. *J. Am. Chem. Soc.* **2006**, *128*, 13305.

(9) Xu, W.; Dong, M.; Gersen, H.; Rauls, E.; Vazquez-Campos, S.; Crego-Calama, M.; Reinhoudth, D. N.; Stensgaard, I.; Laegsgaard, E.; Linderoth, T. R.; Besenbacher, F. *Small* **2007**, *3*, 854.

(10) Nyberg, M.; Odelius, M.; Nilsson, A.; Pettersson, L. G. M. *J. Chem. Phys.* **2003**, *119*, 12577.

(11) Blankenburg, S.; Schmidt, W. G. *Phys. Rev. Lett.* **2007**, *99*, 196107.

(12) Blankenburg, S.; Schmidt, W. G. *Nanotechnology* **2007**, *18*, 424030.

(13) Blankenburg, S.; Schmidt, W. G. *Phys. Rev. B* **2008**, *78*, 233411.

(14) Prins, L. J.; Jong, F. D.; Timmerman, P.; Reinhoudt, D. N. *Nature* **2000**, *408*, 181.

(15) Ishi-i, T.; Crego-Calma, M.; Timmerman, P.; Reinhoudt, D. N.; Shinkai, S. *J. Am. Chem. Soc.* **2002**, *124*, 14631.

(16) Schalley, C. A.; Vögtle, F.; Dötz, K. H. *Templates in Chemistry II*; Springer: Heidelberg, 2005.

(17) Xu, W.; Dong, M.; Gersen, H.; Rauls, E.; Vazquez-Campos, S.; Crego-Calama, M.; Reinhoudth, D. N.; Stensgaard, I.; Laegsgaard, E.; Linderoth, T. R.; Besenbacher, F. *Small* **2008**, *4*, 1620.

(18) Kresse, G.; Furthmüller, J. *Comput. Mater. Sci.* **1996**, *6*, 15.

(19) Perdew, J. P.; Chevary, J. A.; Vosko, S. H.; Jackson, K. A.; Pederson, M. R.; Fiolhais, D. J. S. C. *Phys. Rev. B* **1992**, *46*, 6671.

(20) Kresse, G.; Joubert, D. *Phys. Rev. B* **1999**, *59*, 1758.

(21) Bader, R. F. W. *Atoms in Molecules: A Quantum Theory*; Oxford: New York, 1990.

(22) Jones, G.; Jenkins, S. J.; King, D. A. *Surf. Sci.* **2006**, *600*, L224.

(23) Ortmann, F.; Schmidt, W. G.; Bechstedt, F. *Phys. Rev. B* **2006**, *73*, 205101.

(24) E Rauls, S. B.; Schmidt, W. G. *Surf. Sci.* **2008**, *602*, 2170.

(25) Rauls, E.; Schmidt, W. G. *J. Phys. Chem. C* **2008**, *112*, 11490.

(26) Matta, C. F.; Hernández-Trujillo, J.; Tang, T. H.; Bader, R. F. W. *Chem.—Eur. J.* **2003**, *9*, 1940.

(27) Robertson, K. N.; Knop, O.; Cameron, T. S. *Can. J. Chem.* **2003**, *81*, 727.

(28) Tersoff, J.; Hamann, D. R. *Phys. Rev. B* **1985**, *31*, 805.

JP902337P